JACS
JOURNAL OF THE AMERICAN CHEMICAL SOCIETY

ARTICLE

pubs.acs.org/JACS

Synthesis of Complementary Double-Stranded Helical Oligomers through Chiral and Achiral Amidinium−Carboxylate Salt Bridges and Chiral Amplification in Their Double-Helix Formation

Hiroshi Ito,[†,§] Masato Ikeda,[†,∥] Takashi Hasegawa,[†,‡] Yoshio Furusho,[†,‡] and Eiji Yashima*[,†,‡]

[†]Yashima Super-structured Helix Project, Exploratory Research for Advanced Technology (ERATO), Japan Science and Technology Agency (JST), Japan

[‡]Department of Molecular Design and Engineering, Graduate School of Engineering, Nagoya University, Chikusa-ku, Nagoya 464-8603, Japan

Supporting Information

ABSTRACT: A series of complementary molecular strands from 2-mer to 5-mer that are composed of *m*-terphenyl units bearing chiral/achiral amidine or achiral carboxyl groups linked via Pt(II) acetylide complexes were synthesized by sequential stepwise reactions, and their chiroptical properties on the double-helix formation were investigated by circular dichroism (CD) and ^{1}H NMR spectroscopies. In $CHCl_3$, the "all-chiral" amidine strands consisting of (*R*)- or (*S*)-amidine units formed preferred-handed double helices with the complementary achiral carboxylic acid strands through the amidinium−carboxylate salt bridges, resulting in characteristic induced CDs in the Pt(II) acetylide complex regions, indicating that the chiral substituents on the amidine units biased a helical sense preference. The Cotton effect patterns and intensities were highly dependent on the molecular lengths. The complementary double-helix formation was also explored using the chiral/achiral amidine strands with different sequences in which a chiral amidine unit was introduced at the center (center-chiral) or a terminus (edge-chiral) of the amidine strands. The effect of the sequences of the chiral and achiral amidine units on the amplification of chirality (the "sergeants and soldiers" effect) in the double-helix formation was investigated by comparing the CD intensities with those of the corresponding all-chiral amidine double helices with the same molecular lengths. Variable-temperature CD experiments of the all-chiral and chiral/achiral amidine duplexes demonstrated that the Pt(II)-linked complementary duplexes are dynamic and their chiroptical properties including the chirality transfer from the chiral amidine unit to the achiral amidine ones are significantly affected by the molecular lengths, sequences, and temperatures. On the basis of the above results together with molecular dynamics simulation results, key structural features of the Pt(II)-linked oligomer duplexes and the effect of the chiral/achiral amidine sequences on the amplification of chirality are discussed.

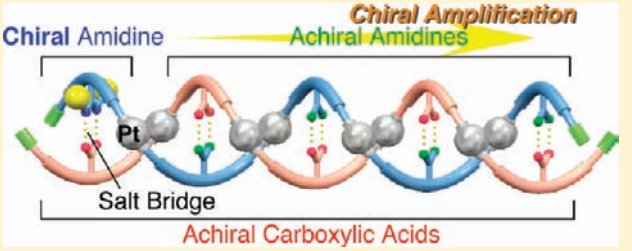

INTRODUCTION

The multiple helix is one of the most fundamental structures in biological macromolecules as observed in nucleic acids, collagen, and polysaccharides, which are spontaneously formed from each component resulting from self-assembly and are closely linked to their exquisite biological functions.[1] For example, α-helices in DNA binding proteins are of vital significance,[1a] and the double-helical DNA efficiently preserves, replicates, and translates the genetic information due to its complementarity in each strand.[1b] Moreover, the collagen's triple helix is critical and of key importance to the fibril formation through a self-assembly process.[1c] Inspired by such sophisticated biological helices, chemists have been challenged to construct artificial multiple-stranded helical structures through self-assembly assisted by noncovalent bonding interactions not only to mimic the structures of biological helices but also to develop chiral materials with a functionality.[2−11] Although a number of synthetic polymers and oligomers (foldamers) which fold into single-handed helical conformations have been reported to date,[2,3] only a limited number of structural motifs and strategies are available for constructing multiple-stranded helical structures,[6g,h] in particular, double-stranded helices.[2v,4] Metal coordination is the most frequently used driving force to construct double, triple, and quadruple helices consisting of metal cations and ligand-containing strands, that is, helicates.[5] Interstrand hydrogen-bonding and aromatic−aromatic interactions have also proved effective for constructing double helices in a few oligoamides[6] and peptide analogues of nucleic acids (peptide nucleic acids (PNAs)).[7]

With the aim of accessing the one handedness in the biological helices, the control of helicity in helicates and PNAs has also been achieved by introducing a chiral substituent into the backbone of the ligand strands or attachment of a chiral residue at

Received: September 21, 2010
Published: February 22, 2011

dx.doi.org/10.1021/ja108514t | *J. Am. Chem. Soc.* 2011, 133, 3419–3432

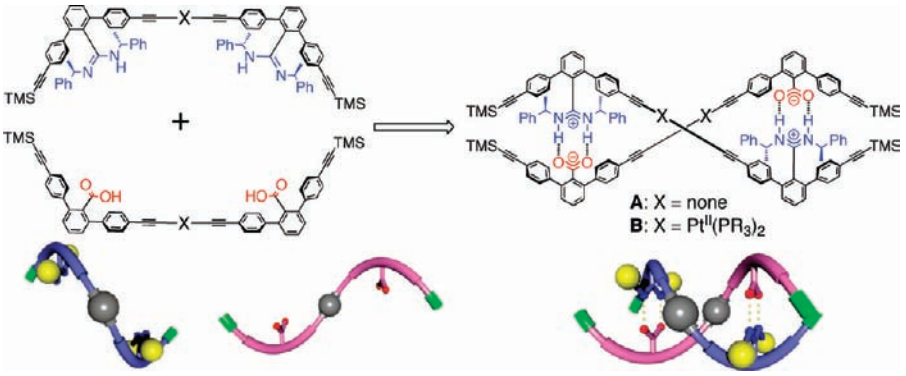

Figure 1. Double-helix formation of complementary chiral amidine 2-mer and achiral carboxylic acid 2-mer.

the terminus or middle of the ligand strands, leading to a helix-sense bias in supramolecular double- or triple-stranded helices.[5b,c,7b−7f] In contrast, enantiomeric multistranded helices showing optical activity due to helicity itself remain quite rare. Spontaneous resolution infrequently yields nonracemic helicates.[5d] The method using chiral auxiliary scaffolds developed by Siegel et al. is a versatile approach to generate enantiomeric double-stranded helicates with an optical activity,[5e−g] involving the transfer of chiral information from the terminal scaffolds to the subsequent achiral ligand strands followed by removal of the scaffold.[12] A similar chirality transfer and succeeding amplification of the helical chirality during double-helix formation have also been observed by Nielsen and co-workers in PNA−PNA duplexes assisted by a chiral residue inserted either at a terminus and/or in the center of an achiral PNA strand.[7]

Recently, we developed a modular strategy to construct complementary artificial double-stranded helices with a controlled helicity stabilized by salt bridges.[11] The helical structure is characterized by crescent-shaped *m*-terphenyl groups with diacetylene linkages and amidinium−carboxylate salt bridges,[11a] and the helix sense of the intertwined two strands is directed by the chirality introduced at the amidine units; duplex **A** (Figure 1) composed of the achiral carboxylic acid strand and chiral amidine strand derived from (*R*)-1-phenylethylamine was revealed to adopt a right-handed double-helical structure as determined by an X-ray crystallographic analysis. By taking advantage of this modular strategy, we linked the *m*-terphenyl units through the *trans*-Pt(II) acetylide moieties, and the Pt(II) complex-containing strands were also proved to produce analogous complementary double helices with an optical activity (R = Ph, **B** in Figure 1) whose helical senses can be biased either by the chiral amidines[11b,c] or by the chiral phosphine ligands attached on the Pt atom connecting the achiral amidine units.[11e]

Metal acetylides complexes, in particular, the Pt(II)−acetylide ones with triethylphosphine ligands, have often been used as effective and variable components for the metal-directed self-assembly to construct supramolecular architectures with well-defined two- and three-dimensional shapes including metallocycles, metallopolyynes, and metallodendrimers because of their synthetic accessibility by the stepwise formation of Pt(II)−acetylides and the kinetic inertness of the robust Pt(II)−alkynyl linkage.[13,14]

In this study, we synthesized a series of chiral amidine strands, from 2-mer to 5-mer, that are composed of (*R*)- or (*S*)-1-phenylethyl and/or achiral isopropyl amidine units with different sequences ((*R*)-**2a**−**5a**, (*R*)-**2b**−**5b**, (*R*)-**3c**, and (*R*)-**5c**), using the Pt(II)−acetylide linkage as a versatile linker via the sequential stepwise reactions, and investigated their double-helix formation with the complementary achiral carboxylic acid strands (**2d**−**4d** and **5e**) and the chain length dependence on the helix-sense bias induction along with the effect of the sequences of the chiral/achiral amidine units on the amplification of the helical chirality in the double-helix formation (the "sergeants and soldiers" effect)[2a,d,15,16] by absorption, circular dichroism (CD), and ^{1}H NMR spectroscopies together with molecular dynamics (MD) simulations (Figure 2).

RESULTS AND DISCUSSION

Synthesis of Oligomers. The chiral and achiral amidine 2-mers ((*R*)- and (*S*)-**2a** and **2f**, respectively) were synthesized by the Cu(I)-catalyzed reaction of $PtCl_2(PEt_3)_2$ and the monoethynyl amidines ((*R*)- and (*S*)-**1a**-H and **1f**-H) with *m*-terphenyl groups, which had been obtained by the monodesilylation of the corresponding amidines ((*R*)- and (*S*)-**1a** and **1f**) (Scheme 1) according to a previously reported method.[11a,c] Treatment of the monoethynyl amidines with an excess of $PtCl_2(PEt_3)_2$ in the presence of CuI and piperidine afforded the monochloroplatinum−acetylide complexes ((*R*)-**1a**-PtCl and **1f**-PtCl) in moderate yields, which were employed as building blocks for the synthesis of the longer oligomers.

The all-chiral amidine strands from 3- to 5-mers ((*R*)-**3a**−**5a**) were prepared in a stepwise manner as shown in Scheme 2. The diethynyl amidine monomer ((*R*)-**1a**-2H) was allowed to react with (*R*)-**1a**-PtCl in the presence of CuI to give the all-chiral 3-mer ((*R*)-**3a**). (*R*)-**2a** and (*R*)-**3a** were treated with tetra-*n*-butylammonium fluoride (TBAF) in THF to afford the diethynyl 2-mer and 3-mer ((*R*)-**2a**-2H and (*R*)-**3a**-2H, respectively), which were further converted to the 4-mer and the 5-mer ((*R*)-**4a** and (*R*)-**5a**, respectively), by the Cu(I)-catalyzed reaction with (*R*)-**1a**-PtCl in the presence of diethylamine.

The edge-chiral amidine strands bearing a chiral amidine unit at the one terminus ((*R*)-**2b**−(*R*)-**5b**) were prepared in a stepwise fashion as shown in Scheme 3. The edge-chiral 2-mer, (*R*)-**2b**, was obtained by the Cu(I)-catalyzed reaction of **1f**-H with (*R*)-**1a**-PtCl. The all-achiral amidine strands with a monoethynyl group (**2f**-H−**4f**-H) were synthesized by the combination of desilylation with TBAF and the Cu(I)-catalyzed coupling reaction with **1f**-PtCl. **2f**-H, **3f**-H, and **4f**-H were then converted to (*R*)-**3b**, (*R*)-**4b**, and (*R*)-**5b**, respectively, by the Cu(I)-catalyzed reaction with (*R*)-**1a**-PtCl.

The center-chiral amidine strands bearing a chiral amidine unit at the center ((*R*)-**3c** and (*R*)-**5c**) were synthesized according to Scheme 4. The chiral amidine with two ethynyl groups at both

dx.doi.org/10.1021/ja108514t | *J. Am. Chem. Soc.* 2011, 133, 3419–3432

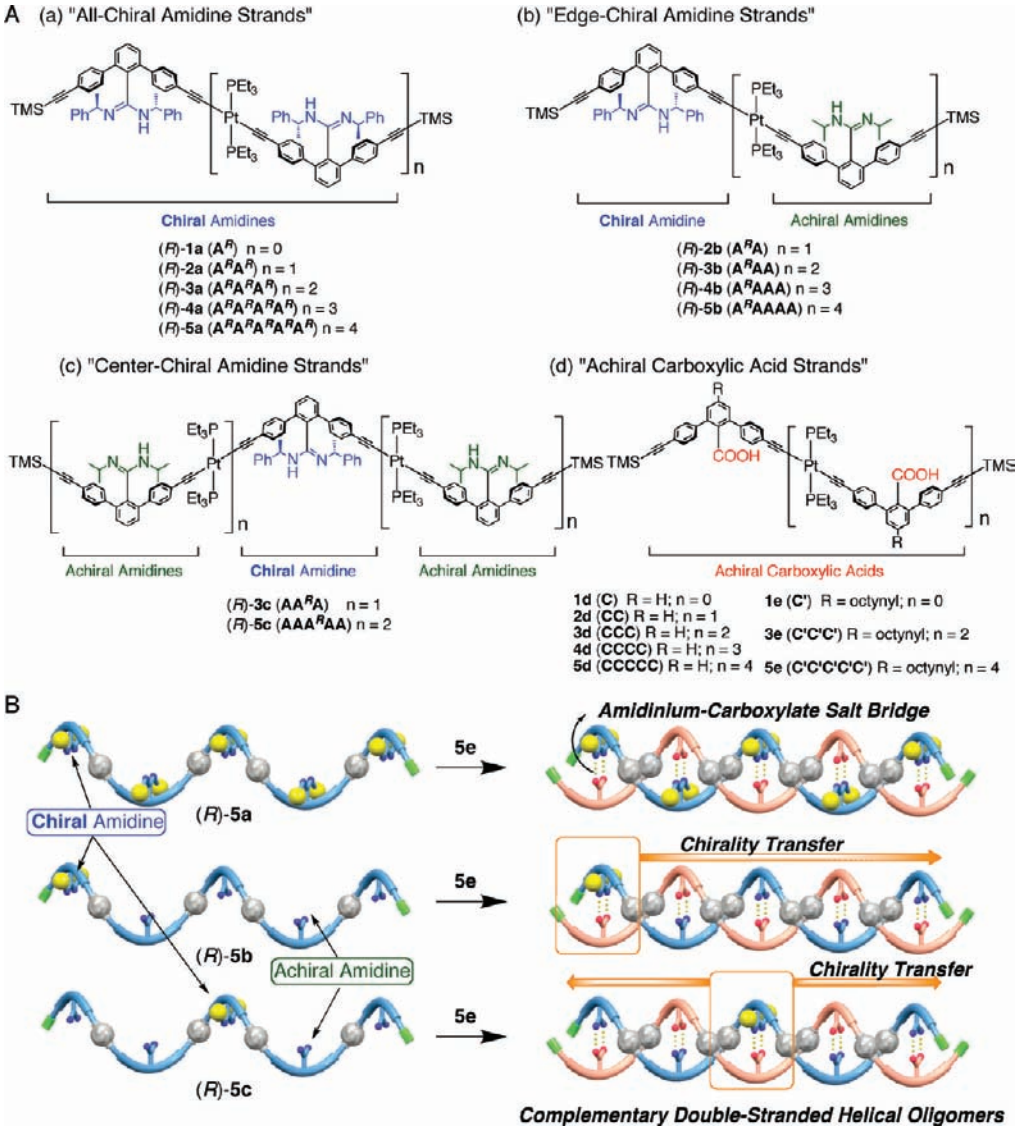

Figure 2. (A) Chiral/achiral amidine strands and achiral carboxylic acid strands synthesized in this study: (a) All-chiral amidine strands; (b) edge-chiral amidine strands; (c) center-chiral amidine strands; (d) achiral carboxylic acid strands. (B) Schematic illustration of chiral amplification in complementary double-stranded helical oligomers (5-mers) composed of chiral/achiral amidine strands and achiral carboxylic acid strands through chirality transfer from the chiral amidine unit at one terminus or at the center.

ends ((*R*)-**1a**-2H) was allowed to react with **1f**-PtCl in the presence of a catalytic amount of CuI to yield (*R*)-**3c**, which was further converted to (*R*)-**5c** by treatment with TBAF followed by reaction with **1f**-PtCl.

The achiral carboxylic acid strands bearing Pt(II)−acetylide linkers (**2d**−**5d** and **5e**) were similarly synthesized to the all-chiral amidine strands (Scheme 5). The monoethynyl carboxylic acid monomer (**1d**-H) was treated with an excess of $PtCl_2(PEt_3)_2$ in the presence of CuI and diethylamine to afford the monochloroplatinum−acetylide complex (**1d**-PtCl). **2d**−**5d** were obtained from **1d**-H by the repetitive procedures of the Cu(I)-catalyzed coupling reaction and desilylation with TBAF. However, an increase in the chain lengths of the oligomers resulted in a drastic solubility decrease, especially for the 5-mer. This problem was overcome by appending a 1-octynyl chain at the "tail" as a solubility enhancer to the carboxylic acid unit. The 5-mer with 1-octynyl chains (**5e**) was prepared from the corresponding 1-mer bearing a 1-octynyl chain at the 5′-position of the *m*-terphenyl group (**1e**-2H) in a manner similar to that for **5d**.

All the oligomers were purified by column chromatography and characterized and identified using ^{1}H and ^{13}C or ^{31}P NMR spectroscopies, elemental analyses, and mass measurements (see the Supporting Information).

Complementary Double-Helix Formation of All-Chiral Amidine Strands with Achiral Carboxylic Acid Strands. First, the double-helix formation of the all-chiral amidine 2-mer ((*R*)-**2a**) and its complementary achiral carboxylic acid 2-mer (**2d**) was investigated by ^{1}H NMR (Figure 3A). Although the ^{1}H NMR spectrum of (*R*)-**2a** in $CDCl_3$ was complicated at 25 °C, because of the presence of several conformers originating from the *E*−*Z* isomerism of the C═N double bonds and the restricted rotation about the C−C bond between the amidine and the *m*-terphenyl groups, the complex (*R*)-**2a**·**2d** showed clear signals, indicating that the geometry around the amidine residues is fixed in the *E*-configuration.[11a] The resonances of the N−H protons (c′) were observed as two broadened doublets at low magnetic fields (13.62 and 13.00 ppm), indicating the salt bridge formation

dx.doi.org/10.1021/ja108514t |*J. Am. Chem. Soc.* 2011, 133, 3419–3432

Scheme 1. Synthesis of Chiral and Achiral Amidine 2-mers

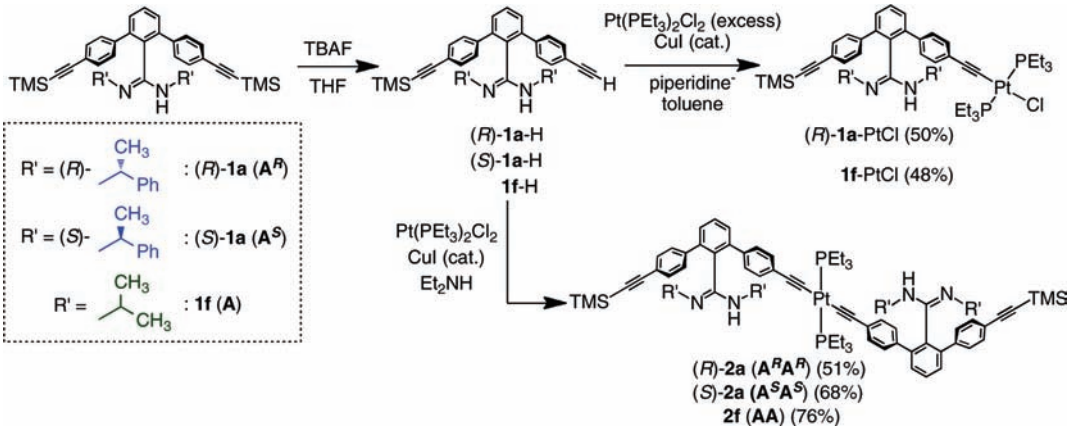

Scheme 2. Synthesis of All-Chiral Amidine Strands[a]

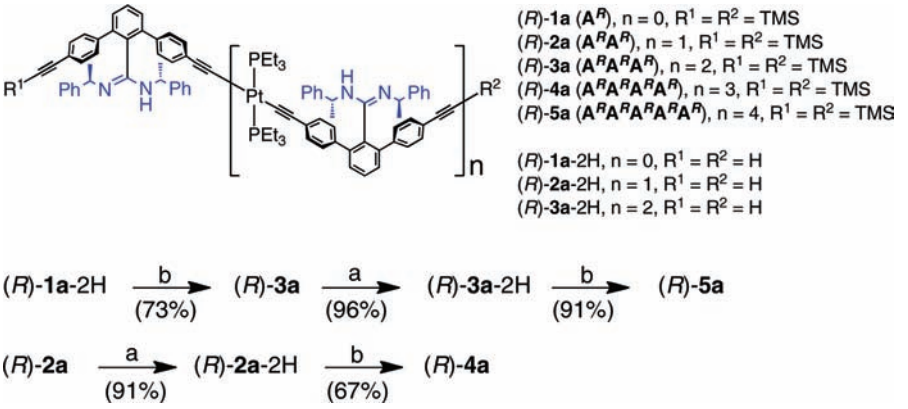

[a] Reagents and conditions: (a) TBAF/THF; (b) (*R*)-**1a**-PtCl, CuI (cat.), $Et_2NH/CHCl_3$.

as well as the molecular motion of the duplex that is slightly restricted probably due to the steric repulsion of the triethylphosphine ligands. Similar but much broadened N−H proton resonances were observed for an analogous duplex bearing triphenylphosphine ligands instead of the triethylphosphine ones as previously reported (**B** in Figure 1; R = Ph).[11b] The methine (a′ and b′) and methyl protons (d′ and f′) of the amidine groups gave two doublets for each. The nonequivalency of these signals is attributed to the double-helical structure of (*R*)-**2a·2d**. The double-helix formation between (*R*)-**2a** and **2d** was also supported by cold-spray ionization (CSI) mass spectrometry (Figure S1A, Supporting Information). The CD spectra of (*R*)-**2a·2d** and (*S*)-**2a·2d** showed intense mirror image CD signals below 380 nm, whereas (*R*)-**2a** and (*S*)-**2a** exhibited very weak Cotton effects (Figure 3B). The significant enhancement of the Cotton effects for (*R*)-**2a·2d** and (*S*)-**2a·2d**, in particular, in the *trans*-Pt(II) acetylide complex region (ca. 300−380 nm), reveals that (*R*)-**2a·2d** and (*S*)-**2a·2d** mostly adopt an excess single-handed double-helical structure as in the case of the diacetylene analogues (**A** and **B** in Figure 1).[11a,b] The association constant (K_a) between (*R*)-**2a** and **2d** in $CDCl_3$ was estimated to be $(5.1 \pm 2.2) \times 10^8\ M^{-1}$ at 25 °C by CD titration experiments (Figure S2, Supporting Information);[17] this K_a value is almost comparable to that of an analogous dimer duplex (**A** in Figure 1).

A series of all-chiral amidine-bound duplexes from 3-mer to 5-mer, (*R*)-**3a·3d**, (*R*)-**4a·4d**, and (*R*)-**5a·5e**, were also prepared by mixing the corresponding all-chiral amidine strands, (*R*)-**3a**, (*R*)-**4a**, and (*R*)-**5a**, and their complementary achiral carboxylic acid strands, **3d**, **4d**, and **5e**.[18] Various attempts to obtain crystals of double-helical oligomers suitable for X-ray analysis including the 2-mers produced only amorphous solids. In addition, the ^1H NMR spectra of the longer duplexes became significantly broadened, although the resonances of the NH protons remained at the low magnetic field of ca. 12−14 ppm, showing that the salt bridges were retained after duplex formation. Therefore, the double-helix formation of the longer oligomers was investigated mainly by CD and absorption spectroscopies (Figure 4A) except for 3-mers (for variable-temperature ^1H NMR spectra for 3-mers, see the text below and Figures S5−S10, Supporting Information). The Cotton effect patterns and intensities in the Pt(II) acetylide complex regions around 300−400 nm were significantly dependent on their molecular length. Among them, the 3-mer ((*R*)-**3a·3d**) showed a rather complicated CD spectrum different from that of the 2-mer (*R*)-**2a·2d**. Surprisingly, a further increase in the molecular length to 4-mer ((*R*)-**4a·4d**) and 5-mer ((*R*)-**5a·5e**) produced inversion of the Cotton effect signs in the Pt(II) acetylide chromophore regions as compared to those of the 2-mer. The (*R*)-**4a·4d** and (*R*)-**5a·5e** duplexes exhibited intense Cotton effects in

dx.doi.org/10.1021/ja108514t | *J. Am. Chem. Soc.* 2011, 133, 3419–3432

Scheme 3. Synthesis of Edge-Chiral Amidine Strands[a]

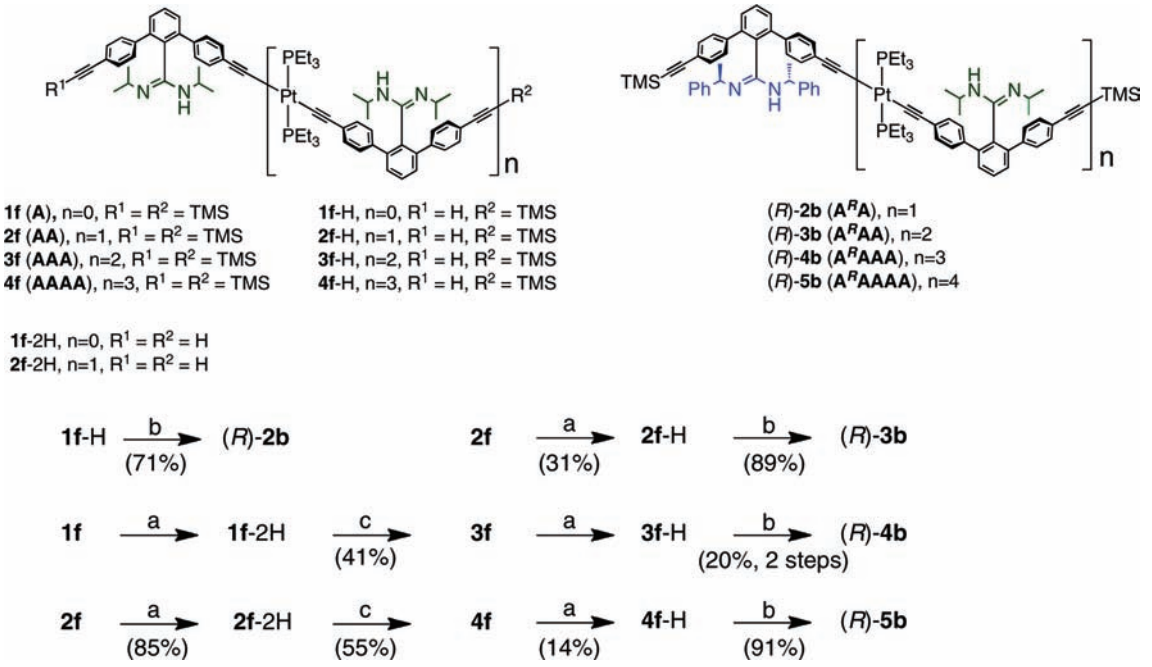

[a] Reagents and conditions: (a) TBAF/THF; (b) (*R*)-**1a**-PtCl, CuI (cat.), $Et_2NH/CHCl_3$; (c) **1f**-PtCl, CuI (cat.), $Et_2NH/CHCl_3$.

the region of 300−400 nm due most likely to the double-helical conformation with a helix-sense bias. These results suggest that the preferred-handed helical sense of the 4- and 5-mers may be opposite to that of the 2-mer, despite the fact that they all have the same (*R*)-phenylethyl groups at the amidine residues (for more detailed studies on the temperature effects on their CD spectral patterns and intensities, see below). As previously reported, such an inversion of the Cotton effects did not take place for the diacetylene-linked fully organic double-helical oligomers.[11g]

In order to gain insight into the mechanism of the Cotton effect inversion depending on the molecular length, we measured the concentration-dependent CD spectral changes of a series of the all-chiral amidine-bound duplexes in $CDCl_3$ at 25 °C. At concentrations higher than ca. 10^{-5} M, the CD intensity of (*R*)-**5a·5e** was found to dramatically decrease while maintaining its Cotton effect pattern (Figure 4B and 4C). This sudden onset and rapid decrease in the optical activity were accompanied by a slight red shift of λ_{max} by ca. 5 nm with a clear isosbestic point at 340 nm (Figure 4B), which suggested that (*R*)-**5a·5e** may change its structure into a rather complex aggregate other than the discrete double helix at high concentrations. Dynamic light scattering (DLS) measurements support formation of a large aggregate, such as a supramolecular double-helical oligomer with a hydrodynamic diameter (D_H) of ca. 300 nm when prepared at 20 μM in $CHCl_3$ (Figure 4D). Upon dilution to 0.2 μM, the D_H value gradually decreased with time and no light scattering due to the aggregate could be observed after 4 days. In addition, this dynamic structural change was accompanied by an increase in the first Cotton effect intensity at 358 nm, resulting in complete recovery of the CD spectrum to that of (*R*)-**5a·5e** prepared at concentrations lower than 10^{-5} M ($\Delta\varepsilon_{358} = 270\ cm^{-1}\ M^{-1}$) after 18 days. These results demonstrate that an equilibrium exists between the double helix and supramolecular aggregates depending on the concentration, and the latter is predominant at high concentrations which readily converts to the double helix at low concentrations, as illustrated in Figure 4E. We note that such a remarkable concentration-dependent CD spectral change was never observed for other smaller duplexes of 2-mer −4-mer except for the edge-chiral amidine-bound 4-mer ((*R*)-**4b·4d**) in $CHCl_3$ at 25 °C (Figure 5).

Chiral Amplification in Double-Helix Formation of Edge- or Center-Chiral Amidine Strands with Achiral Carboxylic Acid Strands. Duplex formation of the edge-chiral 2-mer strand bearing chiral and achiral amidine units ((*R*)-**2b**) with the complementary achiral carboxylic acid 2-mer strand (**2d**) was confirmed by CSI-mass spectrometry (Figure S1B, Supporting Information) and further investigated by ^{1}H NMR (Figure 6). The ^{1}H NMR spectrum of the amidine strand ((*R*)-**2b**) in $CDCl_3$ (Figure 6a) was complicated as in the case of (*R*)-**2a**. In contrast, (*R*)-**2b·2d** showed a set of clear ^{1}H NMR signals (Figure 6b), which were assigned to one isomer by comparing to those of (*R*)-**2a·2d** (Figure 6c) and **2f·2d** (Figure 6d) consisting of the chiral amidine 2-mer and achiral amidine 2-mer complexed with the carboxylic acid 2-mer, respectively. The resonances of the salt bridge N−H protons of the (*R*)-**2b·2d** were observed as two sets of two doublets at 13.54 and 12.98 ppm and at 12.19 and 12.06 ppm, which were assigned to those of the chiral and achiral amidine units, respectively. The nonequivalent signals of the N−H, methine, and methyl protons of the amidine groups again indicate the double-helical structure of (*R*)-**2b·2d**, as in the case of (*R*)-**2a·2d**. The association constant of (*R*)-**2b** and **2d** ($(1.2 \pm 0.2) \times 10^8\ M^{-1}$) estimated in $CHCl_3$ at 25 °C by CD titration experiments was comparable to that of (*R*)-**2a** and **2d** (Figure S3, Supporting Information),[17] which means that replacement of the chiral amidine unit with the achiral one hardly affects the stability of the double helices.

The CD spectral pattern and intensity of (*R*)-**2b·2d** measured at 25 °C are quite similar to those of (*R*)-**2a·2d** (Figure 7A), suggesting that the 2-mers most probably adopt a double-helical structure similar to each other with the same handedness

dx.doi.org/10.1021/ja108514t | *J. Am. Chem. Soc.* 2011, 133, 3419–3432

Scheme 4. Synthesis of Center-Chiral Amidine Strands[a]

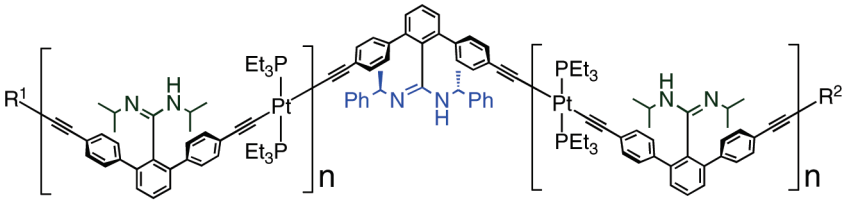

(*R*)-**3c** (**AA^{R}A**), n = 1, $R^1 = R^2$ = TMS
(*R*)-**5c** (**AAA^{R}AA**), n = 2, $R^1 = R^2$ = TMS

(*R*)-**1a**-2H, n = 0, $R^1 = R^2$ = H
(*R*)-**3c**-2H, n = 1, $R^1 = R^2$ = H

(*R*)-**1a**-2H —c (82%)→ (*R*)-**3c** —a (90%)→ (*R*)-**3c**-2H —c (87%)→ (*R*)-**5c**

[a] Reagents and conditions: (a) TBAF/THF; (c) **1f**-PtCl, CuI (cat.), $Et_2NH/CHCl_3$.

and almost the same degree of helix-sense excess, i.e., the (*R*)-phenylethyl groups on one of the amidine residues effectively act as a helix-sense director to induce the same helical sense in the next achiral amidine unit when complexed with **2d** (Figure 8). The chiral/achiral amidine strands longer than 2-mer, (*R*)-**3b**, (*R*)-**3c**, (*R*)-**4b**, (*R*)-**5b**, and (*R*)-**5c**, were then mixed with the complementary achiral carboxylic acid strands in $CHCl_3$ to afford a series of duplexes, (*R*)-**3b·3d**, (*R*)-**3c·3d**, (*R*)-**4b·4d**, (*R*)-**5b·5e**, and (*R*)-**5c·5e**, respectively, which also had a helix-sense bias, as apparent from their CD induction (Figure 7B−D). As observed for the all-chiral amidine-bound 5-mer duplex ((*R*)-**5a·5e**), the 5-mers of (*R*)-**5b·5e** and (*R*)-**5c·5e** bearing one chiral amidine unit at the terminus and center, respectively, also displayed a strong concentration dependence in their double-helix formations (Figure 5). Interestingly, among the other oligomer duplexes, only the edge-chiral amidine-bound 4-mer duplex ((*R*)-**4b·4d**) exhibited a concentration dependence in the double-helix formation, as opposed to the all-chiral amidine-bound 4-mer duplex, which suggests that the double-helix formation over supramolecular aggregations is sensitive to the sequences of the chiral/achiral amidine strands to a certain extent. Therefore, the following CD and absorption measurements for (*R*)-**4b·4d**, (*R*)-**5b·5e**, and (*R*)-**5c·5e** were performed at concentrations as low as 10^{-6} M.

Although the all-chiral amidine-bound 3-mer ((*R*)-**3a·3d**) exhibited a complicated CD spectral pattern different from those of the corresponding 2-, 4-, and 5-mers (see Figure 4A), the edge- ((*R*)-**3b·3d**) and center-chiral ((*R*)-**3c·3d**) amidine-bound 3-mers showed a rather simple and similar positive first Cotton effect in the Pt(II) acetylide chromophore regions with negligible absorbance changes (Figure 7B), suggesting that they may adopt a double helix with the same handedness. The edge- and center-chiral amidine-bound 4-mer and 5-mer duplexes also showed apparent CDs, but their spectral patterns in the Pt(II) linker regions changed from a split-type to nonsplit one, while largely maintaining the positive first Cotton effect (Figure 7C and 7D). In addition, an appreciable difference in the CD intensity depending on the position of the chiral amidine unit was observed for the 5-mers.

Though less quantitative, the CD intensities corresponding to the main-chain chromophore regions most likely reflect the helix-sense excess of the helical oligomers when their CD and absorption spectral patterns are almost identical, thereby allowing a comparison between the helix-sense biases of the oligomers

Scheme 5. Synthesis of Achiral Carboxylic Acid Strands[a]

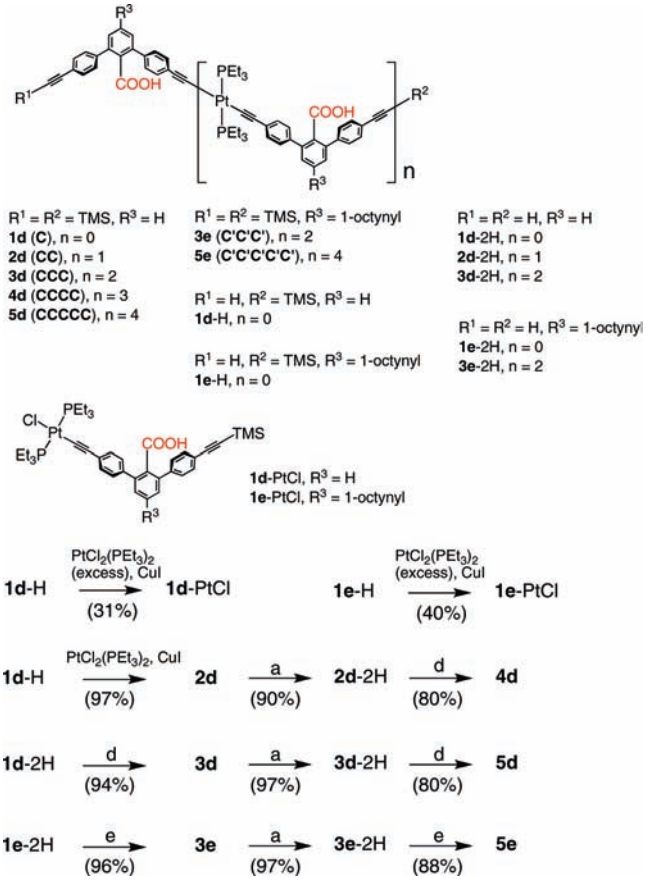

[a] Reagents and conditions: (a) TBAF/THF; (d) **1d**-PtCl, CuI (cat.), $Et_2NH/CHCl_3$; (e) **1e**-PtCl, CuI (cat.), $Et_2NH/CHCl_3$.

with the same chain lengths but different chiral/achiral amidine sequences, because the CD signals of the Pt(II) linker regions do not overlap those of the chiral phenylethyl chromophore region and their chemical structures are quite similar to each other except for the number of chiral/achiral amidine residues. The chiral/achiral hybrid 3-mer duplexes with a chiral unit content less than that of (*R*)-**2b·2d** (50%), (*R*)-**3b·3d**, and (*R*)-**3c·3d** (33%), also showed appreciable Cotton effects whose intensities

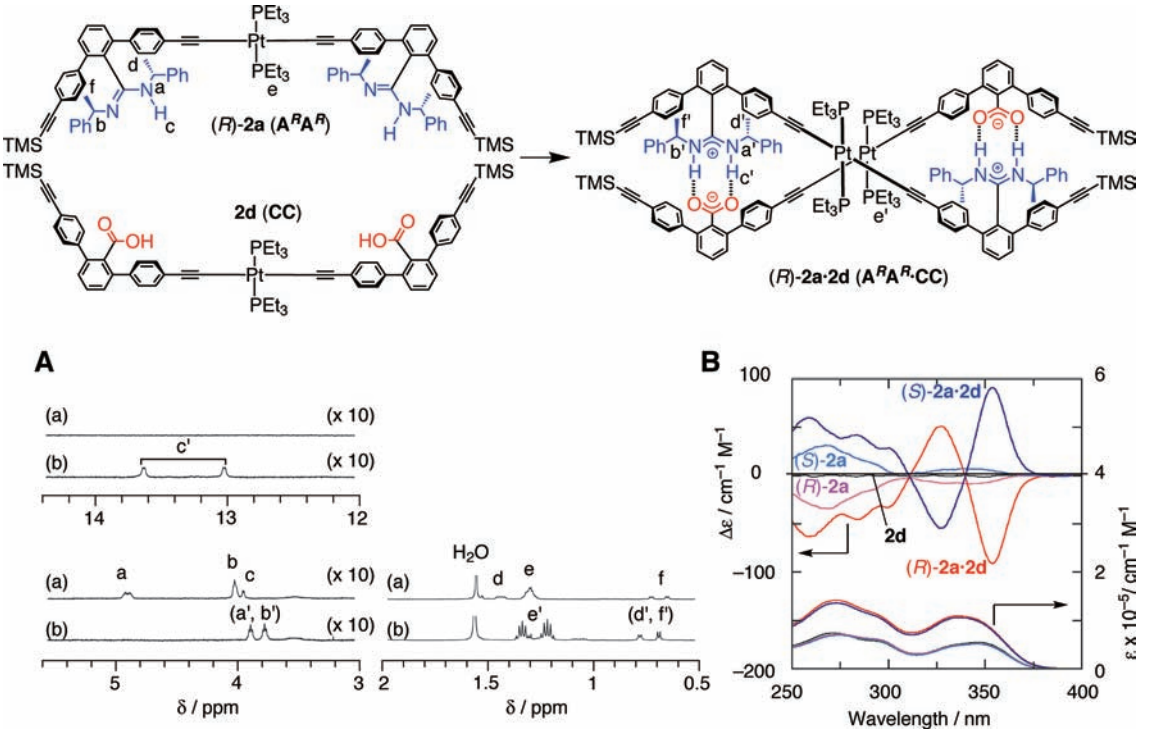

Figure 3. (A) Partial ^{1}H NMR (500 MHz) spectra of (a) (*R*)-**2a** (0.50 mM) in $CDCl_3$ at 25 °C and (b) (*R*)-**2a**·**2d** (0.50 mM). (B) CD and absorption spectra of (*R*)-**2a**, (*S*)-**2a**, (*R*)-**2a**·**2d**, and (*S*)-**2a**·**2d** (0.10 mM) in $CDCl_3$ at 25 °C.

were slightly greater than that of the all-chiral amidine-bound double helix ((*R*)-**3a**·**3d**) (Figures 7B and 8), although different CD spectral patterns hampered the quantitative discussion on the amplification of helical chirality. The edge-chiral amidine-bound 4-mer duplex ((*R*)-**4b**·**4d**), having a chiral unit content of only 25%, also exhibited as an intense CD as that of the all-chiral amidine-bound 4-mer duplex ((*R*)-**4a**·**4d**), implying that the chirality of the terminus amidine unit is transferred to the subsequent achiral amidine units when complexed with the complementary achiral carboxylic acid strand (**4d**), resulting in an excess of the one-handed double helix (Figures 7C and 8). In contrast, the CD intensities for the chiral/achiral hybrid 5-mer duplexes ((*R*)-**5b**·**5e** and (*R*)-**5c**·**5e**) (the chiral amidine content = 20%) decreased by comparison to that of the all-chiral amidine-bound 5-mer double helix ((*R*)-**5a**·**5e**), indicating less efficiency in the chirality transfer during the double-helix formation, especially for the edge-chiral amidine-bound 5-mer ((*R*)-**5b**·**5e**). It should be noted that each complementary carboxylic acid strand is totally achiral, which demonstrates that the chirality transfer or amplification of the chirality indeed takes place along the double-helix formation, although its efficiency is highly dependent on the sequence and oligomer length.

Thus, the chirality amplification in the 5-mers seems to be highly affected by the sequences of the chiral and achiral amidine units, in other words, the position of the chiral amidine unit (Figures 7D and 8). A preferred-handed helical conformation in the double helices may be more efficiently induced by the chiral amidine unit inserted into the middle part of the longer oligomers than that at the terminal part. A similar preference of one-handedness was observed for the PNA−PNA duplexes having an L-amino acid residue in the center of an achiral PNA strand.[7]

Next, we performed variable-temperature CD measurements in order to obtain information on the dynamic properties of the optically active duplex oligomers, which may be closely related to the ability of the chiral amidine residues to transfer its chirality to the double-stranded oligomer backbones in solution. Because longer duplexes, (*R*)-**4b**·**4d** and all the 5-mer duplexes, precipitated at low temperatures in $CHCl_3$ and also in CH_2Cl_2, toluene was chosen as the measuring solvent which enabled CD measurements of all the duplexes at temperatures as low as −80 °C in the same solvent. However, we found unusual solvent and temperature effects on the chiroptical properties of the duplexes except for the 2-mers, which showed almost no solvent- and temperature-dependent CD and absorption spectral changes.[19] The Cotton effect patterns of the longer duplexes (3-mer−5-mer) reversibly changed with lowering temperatures, and their intensities tended to lower in toluene at 25 °C accompanied by inversion of the CD signatures for some oligomers, indicating the dynamic chiroptical properties of the longer double helices (Figures 9 and S4, Supporting Information).[20]

The Cotton effect signs of the all-chiral amidine 3-mer ((*R*)-**3a**·**3d**) were unexpectedly inverted in toluene (Figure 9A), and the CD intensities of the first Cotton effects ($\Delta\varepsilon_{first}$) of all the 3-mers monotonically increased in the negative direction with decreasing temperature (Figure 9A−C) but did not reach a plateau value even at −80 °C as indicated by the plots of the $\Delta\varepsilon_{first}$ values versus temperature (Figure 9D). At low temperatures, the CD spectral patterns for the edge- and center-chiral 3-mer duplexes changed to a split-type one like those of the 2-mers. These changes in their CD spectra were accompanied by a slight increase in their absorbance, suggesting that conformational changes took place at low temperatures. As a consequence, it is difficult to determine the handedness and to quantify the helical sense excesses and the extent of the amplification of helical chirality of the edge- and center-chiral 3-mer duplexes based on the CD profile of the all-chiral 3-mer duplex. However, the fact

dx.doi.org/10.1021/ja108514t |*J. Am. Chem. Soc.* 2011, 133, 3419–3432

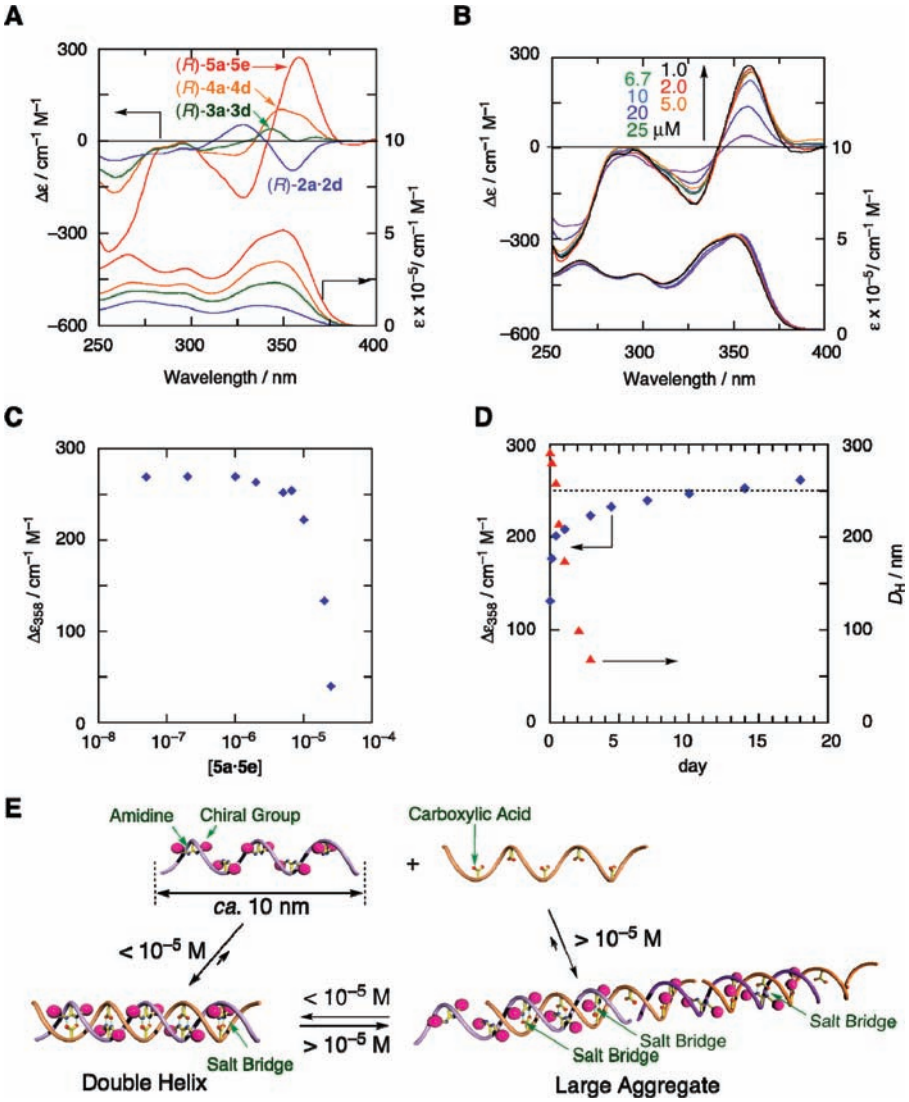

Figure 4. (A) CD and absorption spectra of (*R*)-**2a·2d**, (*R*)-**3a·3d**, (*R*)-**4a·4d**, and (*R*)-**5a·5e** ($CDCl_3$, 1.0 μM, 25 °C). (B) CD and absorption spectra of (*R*)-**5a·5e** prepared at various concentrations (1−25 μM). (C) $\Delta\varepsilon$ values at 358 nm ($\Delta\varepsilon_{358}$) plotted against the concentrations of (*R*)-**5a·5e** (25−0.05 μM). (D) Time course of the changes in the $\Delta\varepsilon_{358}$ and D_H estimated by DLS measurements of a solution of (*R*)-**5a·5e** prepared at 20 μM and subsequently diluted to 0.2 μM. The dotted line represents the $\Delta\varepsilon_{358}$ value of (*R*)-**5a·5e** measured at 2.0 μM at 25 °C. (E) Schematic illustration for the formation of a double helix and a possible large aggregate of (*R*)-**5a** and **5e** depending on the concentrations.

that the temperature-dependent CD intensity change for the center-chiral duplex ((*R*)-**3c·3d**) was comparable to that of the all-chiral 3-mer duplex ((*R*)-**3a·3d**) and larger than that for the edge-chiral 3-mer duplex ((*R*)-**3b·3d**) (Figure 9D) suggests that the double-helical structure with a chiral unit at the middle position may form a more excess one-handed double helix than that with a chiral unit at the end at low temperatures.

Variable-temperature ^{1}H NMR spectra of 3-mers in the temperature range between −50 and 55 °C (Figures S5−S10, Supporting Information) revealed that the all-chiral amidine 3-mer ((*R*)-**3a·3d**) maintained its duplex structure stabilized by the salt bridge formation over the full range of temperatures investigated as supported by the apparent salt bridge NH proton resonances (Figures S5 and S8, Supporting Information), whereas the corresponding NH proton resonances for (*R*)-**3b·3d** and (*R*)-**3c·3d** became significantly broadened at high temperature (Figures S6 and S7, Supporting Information, respectively) and even at low temperature for the edge-chiral 3-mer duplex ((*R*)-**3b·3d**) (Figure S9, Supporting Information). In contrast, the broad salt bridge NH proton signals for the center-chiral duplex ((*R*)-**3c·3d**) slightly sharpened within the temperature range from 0 to −30 °C (Figure S10, Supporting Information), suggesting that (*R*)-**3c·3d** may possess a more stable and regular helical structure relative to (*R*)-**3b·3d** at low temperatures. More significant changes in the variable-temperature ^{1}H NMR spectra were observed for the terminal TMS proton resonances for (*R*)-**3b·3d** and (*R*)-**3c·3d**, which split into broad complicated multiple signals at −30 and −50 °C (Figures S8−S10, Supporting Information). These results indicate the presence of several helical conformations under dynamic equilibrium that may be responsible for their rather complicated CD spectral changes with temperature. Again, the changes in the TMS proton signals at low temperature were significant for the edge-chiral 3-mer duplex ((*R*)-**3b·3d**), implying more complicated helical conformations relative to (*R*)-**3c·3d** as supported by the molecular dynamics (MD) simulation results (see below).

dx.doi.org/10.1021/ja108514t |*J. Am. Chem. Soc.* 2011, 133, 3419–3432

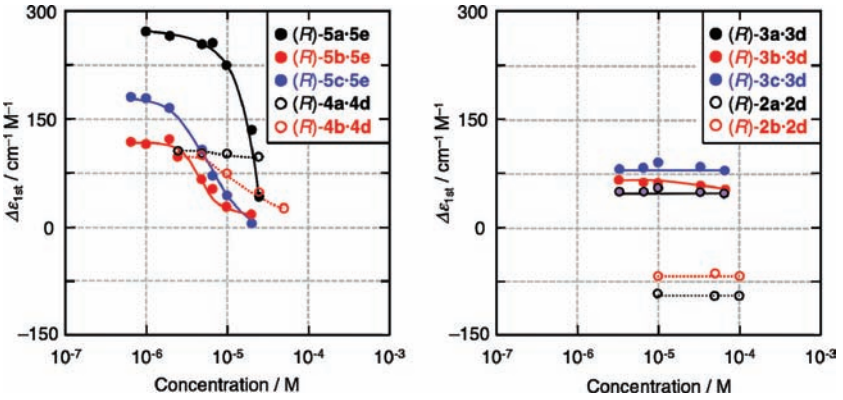

Figure 5. Plots of molar circular dichroism at the first Cotton effect ($\Delta\varepsilon_{first}$) against the concentration of the double-stranded helical oligomers in $CHCl_3$ at 25 °C; (*R*)-**5a·5e** (360 nm), (*R*)-**5b·5e** (358 nm), (*R*)-**5c·5e** (362 nm), (*R*)-**4a·4d** (350 nm), (*R*)-**4b·4d** (357 nm), (*R*)-**3a·3d** (343 nm), (*R*)-**3b·3d** (346 nm), (*R*)-**3c·3d** (345 nm), (*R*)-**2a·2d** (354 nm), and (*R*)-**2b·2d** (357 nm).

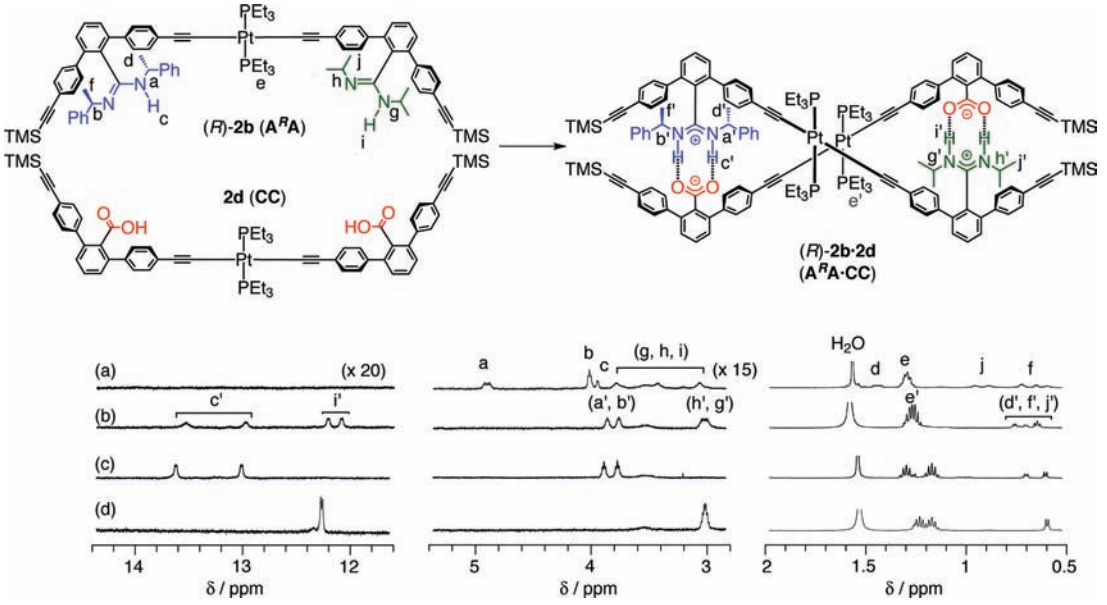

Figure 6. Partial ^{1}H NMR (500 MHz, $CDCl_3$, 25 °C) spectra of (a) (*R*)-**2b** (0.50 mM), (b) (*R*)-**2b·2d** (0.50 mM), (c) (*R*)-**2a·2d** (0.10 mM), and (d) **2f·2d** (0.10 mM).

As for the 4-mers, both the all-chiral and the edge-chiral 4-mers ((*R*)-**4a·4d** and (*R*)-**4b·4d**) also underwent a considerable change in their CD signals in toluene associated with inversion of the Cotton effect signs, although the absorbance spectra showed almost no change during the CD signal inversion (Figure S4A and 4B, Supporting Information). The first positive Cotton effects remained unchanged independent of the temperatures, while the CD signal at the second Cotton effect gradually increased in the negative direction with the decreasing temperature. A comparison of plots of the CD intensities versus temperature (Figure 9E) by taking into account the negligible absorbance change for the 4-mers indicates that the edge-chiral (*R*)-**4b·4d** might possess a double-helical structure similar to that of the (*R*)-**4a·4d**, but a helical sense excess of the edge-chiral (*R*)-**4b·4d** may be lower than that of the all-chiral (*R*)-**4a·4d** to some extent.

The variable-temperature CD profiles for the 5-mer duplexes seem to be more complicated (Figures 9F and S4C−E, Supporting Information). In particular, almost no CD was observed in the Pt(II) linker regions for the edge-chiral 5-mer duplex ((*R*)-**5b·5e**) at 25 °C in toluene (Figure S4D, Supporting Information), most probably because of a reversal in the helical sense due to a solvent effect;[20] a positive first Cotton effect in $CHCl_3$ might change to the opposite, negative Cotton effect in toluene. In fact, a decrease in the temperature resulted in a further increase in the CD intensity in the negative direction, although the CD intensity was still weak as compared to those of the other 5-mers. The all-chiral 5-mer duplex ((*R*)-**5a·5e**) maintained its split-type CD pattern regardless of the temperature, while the second Cotton effect intensity increased with the decreasing temperature accompanied with a remarkable red shift (Figure S4C, Supporting Information). On the other hand, a different behavior was observed for the center-chiral 5-mer duplex ((*R*)-**5c·5e**); the CD signals at the first and second Cotton effects decreased almost by one-half as the temperature was lowered from 25 to −80 °C. We noted that these CD spectral changes

dx.doi.org/10.1021/ja108514t |*J. Am. Chem. Soc.* 2011, 133, 3419–3432

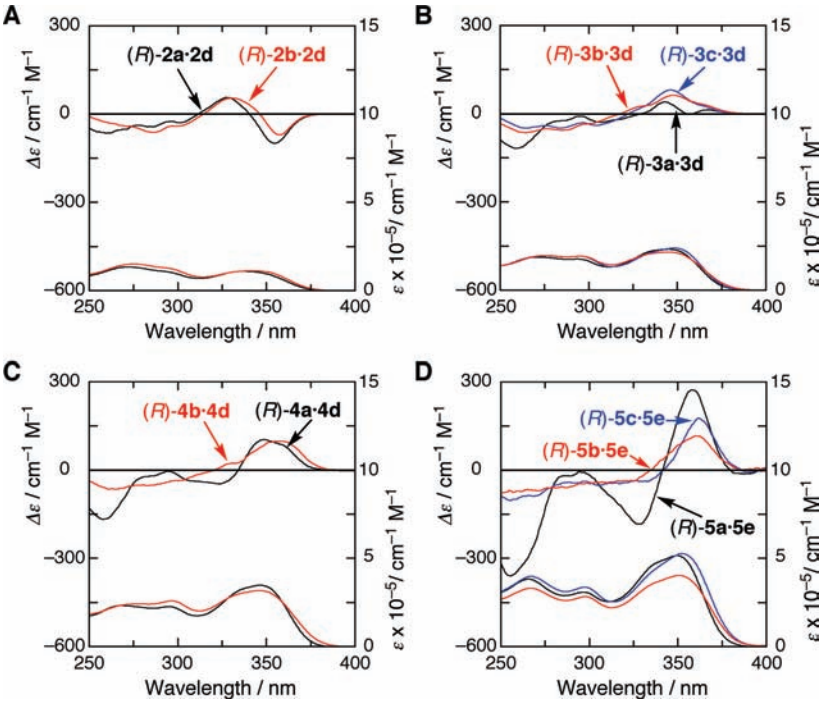

Figure 7. CD and absorption spectra of double-stranded helical oligomers: (A) 2-mers (0.1 mM), (B) 3-mers (0.067 mM), (C) 4-mers (2.5 μM), and (D) 5-mers (1.0 μM) in $CHCl_3$ at 25 °C.

were accompanied by slight increases in their absorbance, indicating that structural changes may not have occurred for all 5-mer duplexes. On the basis of the variable-temperature CD spectral changes of all 5-mer duplexes in toluene (Figure 9F) together with their CD spectra in $CHCl_3$ (Figure 7D), it can be concluded that the chirality of the amidine residue either at the center or the terminus is certainly transferred to the achiral amidine units but its efficiency may be better when the chiral amidine is placed in the center of the amidine strand. A similar tendency was observed for the 3-mer duplexes.

Molecular Dynamics Simulations of 3-mer Duplexes. To gain information regarding the helical structures of longer oligomer duplexes, we performed MD calculations for a series of 3-mers ((*R*)-**3a·3d**, (*R*)-**3b·3d**, and (*R*)-**3c·3d**) using the Universal Force Field.[21] The initial structures were generated on the basis of the structural motif of duplex **A** determined by single-crystal X-ray analysis (Figure 1)[11a] followed by the *trans*-Pt(II) acetylide linkage insertion.[11b] The triethylphosphine ligands of (*R*)-**3a·3d**, (*R*)-**3b·3d**, and (*R*)-**3c·3d** were replaced by trimethylphosphine for facilitating the calculations. The MD calculations were run for the 3-mers for 1 or 10 ns at constant volume and temperature (300, 350, and 400 K) (NVT MD using the Hoover temperature thermostat) with a step size of 1 fs. Figure S11, Supporting Information, shows representative snapshots of the 3-mers along 0.5−1 ns at 125 ps intervals. During the MD simulations for 1 ns at 300−400 K and 10 ns at 300 K, transitional conformations such as helical inversion and dissociation into single strands were not observed, suggesting that a helical conformation may certainly be a favorable conformation for the 3-mer duplexes independent of the chiral/achiral amidine sequences. However, we noticed remarkable changes in the salt bridges of the achiral amidinium−carboxylates depending on their positions (edge or center) (Figure S11 and Table S1, Supporting Information). The salt bridges of the chiral amidinium−carboxylate remain in contact (6.717−7.471 Å) for all the 3-mer duplexes at 300−400 K independently of their sequences, whereas the achiral amidinium−carboxylate salt bridges of (*R*)-**3b·3d** and (*R*)-**3c·3d** significantly increased in length, becoming definitely longer than the adjacent chiral amidinium−carboxylate salt bridge lengths at 300−400 K. More importantly, for the edge-chiral amidine 3-mer ((*R*)-**3b·3d**), the terminal achiral amidinium−carboxylate salt bridge partially dissociates into a single hydrogen bond (Figure S11B, Supporting Information) and its length further elongated (8.982−9.815 Å) as compared with the central one (7.105−7.890 Å) (Table S1, Supporting Information) except in case at 400 K. In addition, one of the two terminal achiral amidinium−carboxylate salt bridges of (*R*)-**3c·3d** (7.164−8.552 Å) was considerably shorter than the other (7.844−9.986 Å) at 300−350 K, while maintaining its double hydrogen bonds. All of these MD simulations suggest that the salt bridges composed of chiral amidines appear to be more rigid and stable than those of the achiral amidines and the achiral amidine-bound salt brides at the strand ends are more flexible than the others, resulting in partial dissociation into single hydrogen bond. Of particular note is the significantly greater flexibility of the terminal achiral amidinium−carboxylate salt bridge of (*R*)-**3b·3d** relative to the corresponding central achiral amidinium−carboxylate salt bridge.

Such key structural features of the 3-mers with different chiral/achiral amidine sequences obtained by the MD simulations appear to be useful in explaining the significant changes in the variable-temperature ^{1}H NMR spectra (Figures S5−S10, Supporting Information) and the temperature-dependent CD spectral changes (Figure 9) for the 3-mers, which may reflect conformational heterogeneity in the 3-mer duplexes most likely due to greater flexibility at the strand ends relative to the center parts, in particular for (*R*)-**3b·3d** and (*R*)-**3c·3d**, and this speculation may be applicable to other longer oligomer

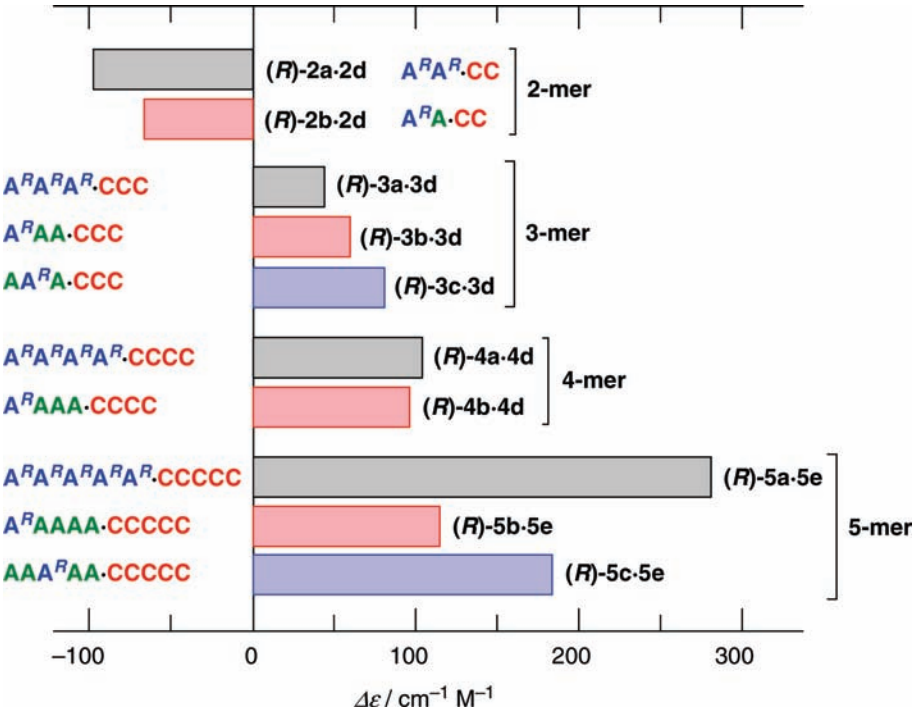

Figure 8. CD intensities of the first Cotton effect of the double helices in $CHCl_3$: (*R*)-**2a·2d** (0.1 mM, 354 nm); (*R*)-**2b·2d** (0.1 mM, 357 nm); (*R*)-**3a·3d** (6.7 μM, 343 nm); (*R*)-**3b·3d** (6.7 μM, 346 nm); (*R*)-**3c·3d** (6.7 μM, 345 nm); (*R*)-**4a·4d** (2.5 μM, 350 nm); (*R*)-**4b·4d** (2.5 μM, 357 nm); (*R*)-**5a·5e** (1.0 μM, 360 nm); (*R*)-**5b·5e** (1.0 μM, 358 nm); (*R*)-**5c·5e** (1.0 μM, 362 nm).

duplexes, leading to unexpected CD and spectral changes with temperature.

■ CONCLUSIONS

We successfully synthesized a series of chiral and chiral/achiral hybrid amidine oligomers with a different sequence and their complementary achiral carboxylic acid oligomers bearing the Pt(II)−acetylide linkages from 2-mer to 5-mer in a stepwise manner utilizing the monochloroplatinum intermediates. The all-chiral amidine oligomers formed intertwined double helices with a helical sense bias when complexed with their complementary carboxylic acid oligomers, as evidenced by the distinct Cotton effects in the absorption regions of the Pt(II) acetylide linkages (ca. 300−380 nm), resulting from the chiral phenylethyl groups on the amidine units, which induced a preferred-handed helical conformation. The Cotton effect signs were unexpectedly dependent on the molecular length, and among the prepared oligomer duplexes, the 2-mer duplexes exhibited an opposite first Cotton effect sign in $CHCl_3$ at 25 °C, suggesting an opposite-handed double-helical structure compared to those of the longer oligomer duplexes. A supramolecular double-helical aggregation took place in relatively highly concentrated solutions for the 5-mer duplexes and the edge-chiral 4-mer duplex. The chiral/achiral hybrid amidine oligomers also formed similar double helices in the presence of the complementary carboxylic acid oligomers, thus showing induced CDs, whose CD patterns and signs were similar to each other when the molecular lengths are the same. Variable-temperature CD experiments of the all-chiral and chiral/achiral oligomer duplexes in a different solvent demonstrate that the Pt(II)-linked duplexes are dynamic and their chiroptical properties are highly sensitive to solvents and temperature as well as molecular lengths and sequences.

Because of the significant changes in the CD spectral patterns and intensities at various temperatures in different solvents for the longer duplexes, quantitative evaluation of the chirality transfer abilities of chiral amidine residues to the achiral ones along the duplex backbones is impossible, but qualitative considerations about the structural and chiroptical properties and chiral amplification in their double-helix formations could be possible on the basis of the detailed systematic experimental results together with the MD simulation results for the 3-mers; the chiral/achiral alternative 2-mer duplex most likely possesses an excess one-handedness comparable to that of the all-chiral amidine 2-mer, since both of the 2-mers exhibited a similar Cotton effect pattern and intensity independent of the solvents and temperature accompanied by negligible absorbance changes, leading to the conclusion that chiral information at the chiral amidine unit probably transfers to the next achiral amidine unit in an efficient fashion. A preferred-handed helical sense excess in the longer duplexes may be more efficiently induced by the chiral amidine unit inserted into the middle part of the oligomers than that at the terminal part. A plausible explanation for this may lie in the Pt(II)−acetylide linkages that likely generate a greater flexibility of the Pt(II)-linked duplexes relative to the fully organic, diacetylene-linked duplexes (**A** in Figure 1).[22] The MD simulations suggest that the chiral amidinium−carboxylate salt bridges may be more rigid and stable than the achiral amidinium−carboxylate ones. In particular, the achiral amidinium−carboxylate salt bridges at the strand ends may be much more flexible than the others, resulting in conformational heterogeneity, which likely reflects the complicated changes in the variable-temperature ^{1}H NMR and CD spectra for longer oligomer duplexes as mentioned above.[23]

In addition, the present study also implies that even fully chiral−amidine duplex oligomers may not have a complete

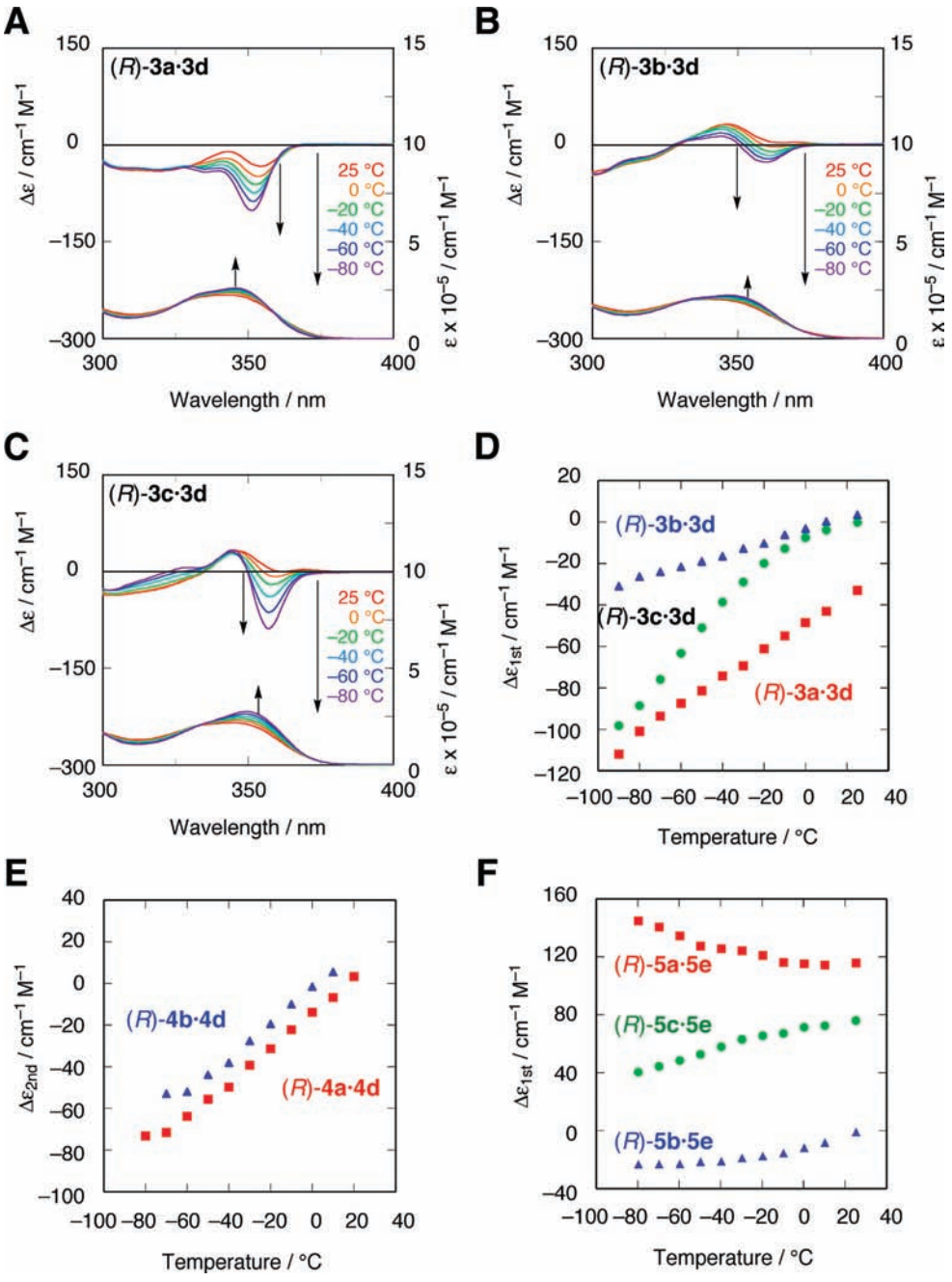

Figure 9. CD and absorption spectra of (*R*)-**3a·3d** (A), (*R*)-**3b·3d** (B), and (*R*)-**3c·3d** (C) in toluene (12.5 μM) at various temperatures. Plots of $\Delta\varepsilon_{first}$ of (*R*)-**3a·3d**, (*R*)-**3b·3d**, and (*R*)-**3c·3d** (D), $\Delta\varepsilon_{second}$ of (*R*)-**4a·4d** and (*R*)-**4b·4d** (E), and $\Delta\varepsilon_{first}$ of (*R*)-**5a·5e**, (*R*)-**5b·5e**, and (*R*)-**5c·5e** (F) against temperature.

one-handed helical conformation with a regular structure except for the 2-mers. Due to the flexibility around the Pt(II) linkers and the duplex ends, a possible reversal in helical sense at the achiral amidine units at the terminus during duplex formation could not be completely excluded. Apparently, a further study on the structural analysis of the Pt(II)-linked duplexes by X-ray is essential to determine the exact helical structure and to obtain more direct evidence dealing with amplification of the helical chirality. Finally, we believe, however, that the present studies would be valuable for the design and synthesis of a wide variety of analogous multistranded helical oligomers and polymers with more stable helical conformations based on amidine−carboxylate salt bridges as unique and specific motifs, providing more sophisticated complementary helical architectures with novel functions.

■ ASSOCIATED CONTENT

Supporting Information. Full experimental details in the synthesis and characterization of the oligomeric strands and the double helices; CSI-mass spectra of (*R*)-**2a·2d** and (*R*)-**2b·2d**, CD titration results of (*R*)-**2a** with **2d** and (*R*)-**2b** and **2d** in $CHCl_3$, variable-temperature CD and absorption spectra of 4-mers and 5-mers in toluene, variable-temperature ^{1}H NMR

dx.doi.org/10.1021/ja108514t | *J. Am. Chem. Soc.* 2011, 133, 3419–3432

spectra of 3-mers in $CDCl_3$, and MD simulation results of 3-mers. This material is available free of charge via the Internet at http://pubs.acs.org.

AUTHOR INFORMATION

Corresponding Author

yashima@apchem.nagoya-u.ac.jp

Present Addresses

[§]Department of Chemistry, Graduate School of Science, Osaka City University.

[‖]Department of Synthetic Chemistry and Biological Chemistry, Graduate School of Engineering, Kyoto University.

ACKNOWLEDGMENT

This work was supported in part by Grant-in-Aid for Scientific Research (S) from the Japan Society for the Promotion of Science (JSPS) and the Japan Science and Technology Agency (JST). We thank Dr. Yoshie Tanaka (JST), Toshihide Hasegawa (JST), and Wataru Makiguchi (Nagoya University) for their help in the synthesis of the starting materials. We also thank Shinzo Kobayashi and Hidekazu Yamada (Nagoya University) for their help in the variable-temperature CD and NMR measurements.

REFERENCES

(1) (a) Branden, C.; Tooze, J. *Introduction to Protein Structure*, 2nd ed.; Garland: New York, 1999. (b) Saenger, W. *Principles of Nucleic Acid Structure*; Springer-Verlag: New York, 1984. (c) Murray, R. K.; Granner, D. K.; Mayes, P. A.; Rodwell, V. W. *Harper's Biochemistry*, 26th ed.; McGraw-Hill: New York, 2003.

(2) For reviews on synthetic polymers and oligomers with single helical conformations, see: (a) Green, M. M.; Peterson, N. C.; Sato, T.; Teramoto, A.; Cook, R.; Lifson, S. *Science* **1995**, *268*, 1860–1866. (b) Gellman, S. H. *Acc. Chem. Res.* **1998**, *31*, 173–180. (c) Rowan, A. E.; Nolte, R. J. M. *Angew. Chem., Int. Ed.* **1998**, *37*, 63–68. (d) Green, M. M.; Park, J.-W.; Sato, T.; Teramoto, A.; Lifson, S.; Selinger, R. L. B.; Selinger, J. V. *Angew. Chem., Int. Ed.* **1999**, *38*, 3139–3154. (e) Brunsveld, L.; Folmer, B. J. B.; Meijer, E. W.; Sijbesma, R. P. *Chem. Rev.* **2001**, *101*, 4071–4097. (f) Cornelissen, J. J. L. M.; Rowan, A. E.; Nolte, R. J. M.; Sommerdijk, N. A. J. M. *Chem. Rev.* **2001**, *101*, 4039–4070. (g) Fujiki, M. *Macromol. Rapid Commun.* **2001**, *22*, 539–563. (h) Hill, D. J.; Mio, M. J.; Prince, R. B.; Hughes, T. S.; Moore, J. S. *Chem. Rev.* **2001**, *101*, 3893–4011. (i) Nakano, T.; Okamoto, Y. *Chem. Rev.* **2001**, *101*, 4013–4038. (j) Nomura, R.; Nakako, H.; Masuda, T. *J. Mol. Catal. A: Chem.* **2002**, *190*, 197–205. (k) Yashima, E.; Maeda, K.; Nishimura, T. *Chem. —Eur. J.* **2004**, *10*, 42–51. (l) Lam, J. W. Y.; Tang, B. Z. *Acc. Chem. Res.* **2005**, *38*, 745–754. (m) Maeda, K.; Yashima, E. *Top. Curr. Chem.* **2006**, *265*, 47–88. (n) Inai, Y.; Komori, H.; Ousaka, N. *Chem. Rec.* **2007**, *7*, 191–202. (o) Kim, H.-J.; Lim, Y.-B.; Lee, M. *J. Polym. Sci., Part A: Polym. Chem.* **2008**, *46*, 1925–1935. (p) Pijper, D.; Feringa, B. L. *Soft Matter* **2008**, *4*, 1349–1372. (q) Rudick, J. G.; Percec, V. *Acc. Chem. Res.* **2008**, *41*, 1641–1652. (r) Yashima, E.; Maeda, K. *Macromolecules* **2008**, *41*, 3–12. (s) Yashima, E.; Maeda, K.; Furusho, Y. *Acc. Chem. Res.* **2008**, *41*, 1166–1180. (t) Kumaki, J.; Sakurai, S.-i.; Yashima, E. *Chem. Soc. Rev.* **2009**, *38*, 737–746. (u) Liu, J.; Lam, J. W. Y.; Tang, B. Z. *Chem. Rev.* **2009**, *109*, 5799–5867. (v) Yashima, E.; Maeda, K.; Iida, H.; Furusho, Y.; Nagai, K. *Chem. Rev.* **2009**, *109*, 6102–6211.

(3) In *Foldamers—Structure, Properties, and Applications*; Hecht, S., Huc, I., Eds.; Wiley-VCH: Weinheim, Germany, 2007.

(4) For reviews on synthetic double helices, see: (a) Lehn, J. M. *Supramolecular Chemistry: Concepts and Perspectives*; VCH: Weinheim, Germany, 1995. (b) Albrecht, M. *Chem. Rev.* **2001**, *101*, 3457–3497. (c) Huc, I. *Eur. J. Org. Chem.* **2004**, 17–29. (d) Furusho, Y.; Yashima, E. *J. Synth. Org. Chem., Jpn.* **2007**, *65*, 1121–1133. (e) Furusho, Y.; Yashima, E. *Chem. Rec.* **2007**, *7*, 1–11. (f) Amemiya, R.; Yamaguchi, M. *Org. Biomol. Chem.* **2008**, *6*, 26–35. (g) Yashima, E.; Maeda, K.; Furusho, Y. *Acc. Chem. Res.* **2008**, *41*, 1166–1180. (h) Furusho, Y.; Yashima, E. *J. Polym. Sci., Part A: Polym. Chem.* **2009**, *47*, 5195–5207. (i) Haldar, D.; Schmuck, C. *Chem. Soc. Rev.* **2009**, *38*, 363–71.

(5) For examples of helicates, see: (a) Lehn, J. M.; Rigault, A.; Siegel, J.; Harrowfield, J.; Chevrier, B.; Moras, D. *Proc. Natl. Acad. Sci. U.S.A.* **1987**, *84*, 2565–2569. (b) Koert, U.; Harding, M. M.; Lehn, J. M. *Nature* **1990**, *346*, 339–342. (c) Zarges, W.; Hall, J.; Lehn, J. M.; Bolm, C. *Helv. Chim. Acta* **1991**, *74*, 1843–1852. (d) Kramer, R.; Lehn, J. M.; De Cian, A.; Fischer, J. *Angew. Chem., Int. Ed. Engl.* **1993**, *32*, 703–706. (e) Woods, C. R.; Benaglia, M.; Cozzi, F.; Siegel, J. S. *Angew. Chem., Int. Ed. Engl.* **1996**, *35*, 1830–1833. (f) Annunziata, R.; Benaglia, M.; Cinquini, M.; Cozzi, F.; Woods, C. R.; Siegel, J. S. *Eur. J. Org. Chem.* **2001**, 173–180. (g) Orita, A.; Nakano, T.; An, D. L.; Tanikawa, K.; Wakamatsu, K.; Otera, J. *J. Am. Chem. Soc.* **2004**, *126*, 10389–10396. (h) Katagiri, H.; Miyagawa, T.; Furusho, Y.; Yashima, E. *Angew. Chem., Int. Ed.* **2006**, *45*, 1741–1744. (i) Miwa, K.; Furusho, Y.; Yashima, E. *Nat. Chem.* **2010**, *2*, 444–449.

(6) For examples of aromatic oligoamides that fold into double helices, see: (a) Berl, V.; Huc, I.; Khoury, R. G.; Krische, M. J.; Lehn, J.-M. *Nature* **2000**, *407*, 720–723. (b) Berl, V.; Huc, I.; Khoury, R. G.; Lehn, J.-M. *Chem.—Eur. J.* **2001**, *7*, 2810–2820. (c) Dolain, C.; Zhan, C.; Leger, J.-M.; Daniels, L.; Huc, I. *J. Am. Chem. Soc.* **2005**, *127*, 2400–2401. (d) Haldar, D.; Jiang, H.; Leger, J.-M.; Huc, I. *Angew. Chem., Int. Ed.* **2006**, *45*, 5483–5486. (e) Zhan, C.; Leger, J.-M.; Huc, I. *Angew. Chem., Int. Ed.* **2006**, *45*, 4625–4628. (f) Berni, E.; Kauffmann, B.; Bao, C.; Lefeuvre, J.; Bassani, D. M.; Huc, I. *Chem. —Eur. J.* **2007**, *13*, 8463–8469. (g) Gan, Q.; Bao, C.; Kauffmann, B.; Grelard, A.; Xiang, J.; Liu, S.; Huc, I.; Jiang, H. *Angew. Chem., Int. Ed.* **2008**, *47*, 1715–1718. (h) Ferrand, Y.; Kendhale, A. M.; Garric, J.; Kauffmann, B.; Huc, I. *Angew. Chem., Int. Ed.* **2010**, *49*, 1778–1781.

(7) For reviews and leading examples of PNA, see: (a) Nielsen, P. E.; Egholm, M.; Berg, R. H.; Buchardt, O. *Science* **1991**, *254*, 1497–1500. (b) Wittung, P.; Nielsen, P. E.; Buchardt, O.; Egholm, M.; Norden, B. *Nature* **1994**, *368*, 561–563. (c) Wittung, P.; Eriksson, M.; Lyng, R.; Nielsen, P. E.; Norden, B. *J. Am. Chem. Soc.* **1995**, *117*, 10167–10173. (d) Nielsen, P. E. *Acc. Chem. Res.* **1999**, *32*, 624–630. (e) Sforza, S.; Haaima, G.; Marchelli, R.; Nielsen, P. E. *Eur. J. Org. Chem.* **1999**, 197–204. (f) Totsingan, F.; Jain, V.; Bracken, W. C.; Faccini, A.; Tedeschi, T.; Marchelli, R.; Corradini, R.; Kallenbach, N. R.; Green, M. M. *Macromolecules* **2010**, *43*, 2692–2703.

(8) For examples of anion-templated double helices, see: (a) Sánchez-Quesada, J.; Seel, C.; Prados, P.; de Mendoza, J.; Dalcol, I.; Giralt, E. *J. Am. Chem. Soc.* **1996**, *118*, 277–278. (b) Keegan, J.; Kruger, P. E.; Nieuwenhuyzen, M.; O'Brien, J.; Martin, N. *Chem. Commun.* **2001**, 2192–2193. (c) Coles, S. J.; Frey, J. G.; Gale, P. A.; Hursthouse, M. B.; Light, M. E.; Navakhun, K.; Thomas, G. L. *Chem. Commun.* **2003**, 568–569.

(9) For helicene-based double helices, see:(a) Sugiura, H.; Nigorikawa, Y.; Saiki, Y.; Nakamura, K.; Yamaguchi, M. *J. Am. Chem. Soc.* **2004**, *126*, 14858–14864. (b) Sugiura, H.; Yamaguchi, M. *Chem. Lett.* **2007**, *36*, 58–59. (c) Amemiya, R.; Saito, N.; Yamaguchi, M. *J. Org. Chem.* **2008**, *73*, 7137–7144. (d) Sugiura, H.; Amemiya, R.; Yamaguchi, M. *Chem.—Asian J.* **2008**, *3*, 244–260.

(10) For poly- and oligo(*m*-phenylene)-based double helices, see: (a) Goto, H.; Katagiri, H.; Furusho, Y.; Yashima, E. *J. Am. Chem. Soc.* **2006**, *128*, 7176–7178. (b) Goto, H.; Furusho, Y.; Yashima, E. *J. Am. Chem. Soc.* **2007**, *129*, 9168–9174. (c) Goto, H.; Furusho, Y.; Yashima, E. *J. Am. Chem. Soc.* **2007**, *129*, 109–112. (d) Ben, T.; Goto, H.; Miwa, K.; Goto, H.; Morino, K.; Furusho, Y.; Yashima, E. *Macromolecules* **2008**, *41*, 4506–4509. (e) Ben, T.; Furusho, Y.; Goto, H.; Miwa, K.; Yashima, E. *Org. Biomol. Chem.* **2009**, *7*, 2509–2512. (f) Goto, H.; Furusho, Y.; Miwa, K.; Yashima, E. *J. Am. Chem. Soc.* **2009**, *131*, 4710–4719.

(11) For artificial double helices based on amidinium—carboxylate salt bridges, see: (a) Tanaka, Y.; Katagiri, H.; Furusho, Y.; Yashima, E.

Angew. Chem., Int. Ed. **2005**, *44*, 3867–3870. (b) Furusho, Y.; Tanaka, Y.; Yashima, E. *Org. Lett.* **2006**, *8*, 2583–2586. (c) Ikeda, M.; Tanaka, Y.; Hasegawa, T.; Furusho, Y.; Yashima, E. *J. Am. Chem. Soc.* **2006**, *128*, 6806–6807. (d) Furusho, Y.; Tanaka, Y.; Maeda, T.; Ikeda, M.; Yashima, E. *Chem. Commun.* **2007**, 3174–3176. (e) Hasegawa, T.; Furusho, Y.; Katagiri, H.; Yashima, E. *Angew. Chem., Int. Ed.* **2007**, *46*, 5885–5888. (f) Katagiri, H.; Tanaka, Y.; Furusho, Y.; Yashima, E. *Angew. Chem., Int. Ed.* **2007**, *46*, 2435–2439. (g) Ito, H.; Furusho, Y.; Hasegawa, T.; Yashima, E. *J. Am. Chem. Soc.* **2008**, *130*, 14008–14015. (h) Maeda, T.; Furusho, Y.; Sakurai, S.-I.; Kumaki, J.; Okoshi, K.; Yashima, E. *J. Am. Chem. Soc.* **2008**, *130*, 7938–7945. (i) Iida, H.; Shimoyama, M.; Furusho, Y.; Yashima, E. *J. Org. Chem.* **2010**, *75*, 417–423. (j) Yamada, H.; Furusho, Y.; Ito, H.; Yashima, E. *Chem. Commun.* **2010**, *46*, 3487–3489.

(12) This template strategy has also been used for preparing fully organic double helical ladders and cyclophanes, see: (a) Nozaki, K.; Terakawa, T.; Takaya, H.; Hiyama, T. *Angew. Chem., Int. Ed.* **1998**, *37*, 131–133. (b) An, D. L.; Nakano, T.; Orita, A.; Otera, J. *Angew. Chem., Int. Ed.* **2002**, *41*, 171–173.

(13) For reviews on Pt(II)−acetylide complexes, see: (a) Stang, P. J.; Olenyuk, B. *Acc. Chem. Res.* **1997**, *30*, 502–518. (b) Yam, V. W.-W. *Acc. Chem. Res.* **2002**, *35*, 555–563. (c) Onitsuka, K.; Takahashi, S. *Top. Curr. Chem.* **2003**, *228*, 39–63. (d) Szafert, S.; Gladysz, J. A. *Chem. Rev.* **2006**, *106*, PR1–PR33.

(14) For examples of unsymmetrical Pt(II)-acetylide complexes synthesized via halo(ethynyl)Pt(II) complexes, see: (a) Leininger, S.; Stang, P. J.; Huang, S. *Organometallics* **1998**, *17*, 3981–3987. (b) Ohshiro, N.; Takei, F.; Onitsuka, K.; Takahashi, S. *J. Organomet. Chem.* **1998**, *569*, 195–202. (c) Onitsuka, K.; Fujimoto, M.; Ohshiro, N.; Takahashi, S. *Angew. Chem., Int. Ed.* **1999**, *38*, 689–692. (d) D'Amato, R.; Furlani, A.; Colapietro, M.; Portalone, G.; Casalboni, M.; Falconieri, M.; Russo, M. V. *J. Organomet. Chem.* **2001**, *627*, 13–22. (e) Yam, V. W.-W.; Tao, C.-H.; Zhang, L.; Wong, K. M.-C.; Cheung, K.-K. *Organometallics* **2001**, *20*, 453–459. (f) Desroches, C.; Lopes, C.; Kessler, V.; Parola, S. *Dalton Trans.* **2003**, 2085–2092. (g) Vives, G.; Carella, A.; Launay, J.-P.; Rapenne, G. *Chem. Commun.* **2006**, 2283–2285. (h) Vives, G.; Carella, A.; Sistach, S.; Launay, J.-P.; Rapenne, G. *New J. Chem.* **2006**, *30*, 1429–1438.

(15) Green, M. M.; Reidy, M. P.; Johnson, R. J.; Darling, G.; Oleary, D. J.; Willson, G. *J. Am. Chem. Soc.* **1989**, *111*, 6452–6454.

(16) For leading references of a preferred-handed helicity induction in helical polymers and oligomers biased by covalently or noncovalently incorporating chiral residues at the chain ends ("domino effect"), see ref 2n and (a) Okamoto, Y.; Matsuda, M.; Nakano, T.; Yashima, E. *Polym. J.* **1993**, *25*, 391–396. (b) Obata, K.; Kabuto, C.; Kira, M. *J. Am. Chem. Soc.* **1997**, *119*, 11345–11346. (c) Inai, Y.; Tagawa, K.; Takasu, A.; Hirabayashi, T.; Oshikawa, T.; Yamashita, M. *J. Am. Chem. Soc.* **2000**, *122*, 11731–11732. (d) Prince, R. B.; Moore, J. S.; Brunsveld, L.; Meijer, E. W. *Chem.−Eur. J.* **2001**, *7*, 4150–4154. (e) Dolain, C.; Jiang, H.; Leger, J. M.; Guionneau, P.; Huc, I. *J. Am. Chem. Soc.* **2005**, *127*, 12943–12951. (f) Pijper, D.; Feringa, B. *Angew. Chem., Int. Ed.* **2007**, *46*, 3693–3696. (g) Abe, H.; Murayama, D.; Kayamori, F.; Inouye, M. *Macromolecules* **2008**, *41*, 6903–6909. (h) King, E. D.; Tao, P.; Sanan, T. T.; Hadad, C. M.; Parquette, J. R. *Org. Let.* **2008**, *10*, 1671–1674.

(17) Connors, K. A. *Binding Constants: The Measurements of Molecular Complex Stability*; John Wiley & Sons, Inc.: New York, 1987.

(18) The 5-mer (**5e**) with 1-octynyl chains was employed because of the poor solubility of the 5-mer (**5d**) in $CHCl_3$, which hampered any further investigation.

(19) In contrast, an analogous 2-mer duplex composed of all-achiral amidine and carboxylic acid strands bearing (*R*)- or (*S*)-2-diphenylphosphino-2′-methoxy-1,1′-binaphthyl (MOP) and triphenylphosphine ligands instead of the triethylphosphine ones at the Pt(II) linkages, respectively, showed a dramatic solvent effect, and its CD intensity significantly increased with the decreasing temperature. In addition, the Cotton effect signs in $CHCl_3$ were almost inverted in toluene at low temperatures, probably because of the steric repulsion caused by the bulky phosphine ligands that may readily assist with the interconversion between the diastereomeric right- and left-handed double helices in solution. See ref 11e.

(20) Solvents are known to affect the stability, conformation, helical sense, and excess helical handedness of some specific single- and double-stranded helical polymers and oligomers. See refs 2d,2j,2l,2s−2v,7f,11e and 16e.

(21) (a) Rappé, A. K.; Casewit, C. J.; Colwell, K. S.; Goddard, W. A., III; Skiff, W. M. *J. Am. Chem. Soc.* **1992**, *114*, 10024–10035. (b) Casewit, C. J.; Colwell, K. S.; Rappé, A. K. *J. Am. Chem. Soc.* **1992**, *114*, 10035–10046. (c) Casewit, C. J.; Colwell, K. S.; Rappé, A. K. *J. Am. Chem. Soc.* **1992**, *114*, 10046–10053.

(22) Diacetylene-linked all-chiral (*R*)-amidine 2-, 3-, and 4-mers formed stable right-handed double-helical structures with their complementary diacetylene-linked carboxylic acid strands in $CHCl_3$ as supported by the no temperature-dependent CD and absorption spectral changes and the X-ray crystal structural analysis for the 2-mer. Moreover, these duplexes, when mixed in solution, could be separated by size-exclusion chromatography, leading to a unique chain-length-specific sorting. See ref 11a and 11g.

(23) Similar conformational heterogeneity has been proposed in PNA−PNA duplexes with a chiral residue at a terminus of an achiral PNA strand; see ref 7f.